Supporting Information

Zarpellon et al. 10.1073/pnas.1017042108

SI Methods.

Expression, Purification, and Characterization of GPIbα-N. The full-length human TPST-2 cDNA coexpressed with the cDNA coding for the human GPIbα fragment −2 to 290 with the Cys^{65} → Ala substitution was cloned into the *Drosophila melanogaster* expression vector pMT/BiP/V5-HisA (Invitrogen, Carlsbad, CA). Site-directed mutagenesis for expressing mutant GPIbα-N, including all Tyr → Phe substitutions, was performed by polymerase chain reaction using oligonucleotide primers containing the desired mutation(s) (QuickChange Site-Directed Mutagenesis Kit, Stratagene, La Jolla, CA). All GPIbα-N species were purified by ion exchange and gel permeation chromatography. To demonstrate differences in sulfate content, duplicate 40 to 100 μg aliquots of each species were equilibrated with 0.05 M sodium acetate, pH 5.5; one was mixed with 60 μg of abalone sulfatase (type VIII; Sigma-Aldrich Co., St. Louis, MO) and both were placed in a heating block at 37 °C. After various incubation times, the reaction was stopped by placing the tubes on ice for 30 min followed by dilution in phosphate-buffered saline. Sulfate removal was analyzed by comparative ion exchange chromatography and isoelectric focusing; the latter was performed with 5 μg of protein in 5% polyacrylamide-2% ampholytes (pH 3–10) applying 100 V for 1 h, 200 V for 1 h, and 500 V for 30 min. Gels were then fixed and proteins stained with Coomassie Blue.

Crystallization of the Complex of Fully Sulfated GPIbα-N with FIIa. Human FIIa was treated with a 25-fold molar excess of PPACK (both from Haematologic Technologies) for eight hours at 22–25 °C and three days at 4 °C. Catalytically blocked FIIa was separated from free inhibitor by gel permeation chromatography (GPC) on a PD10 column (GE Healthcare, Buckinghamshire, United Kingdom) equilibrated with a buffer composed of 20 mM Hepes, 135 mM NaCl, pH 7.4 [Hepes-buffered saline, (HBS)]. Residual proteolytic activity was assessed from the clotting time of a 4 mg/mL fibrinogen solution mixed with 0.1 mg/mL P-FIIa in the presence of 2 mM $CaCl_2$; it was less than 1:1,000,000 of that of untreated FIIa. The complex of GPIbα-N with three Tys residues and P-FIIa was obtained and crystallized as described (1). In brief, the two proteins were mixed at 1:1 molar ratio and the resulting complex was purified by GPC, concentrated to 20 mg/mL in HBS, and crystallized by the hanging drop technique mixing 1 μL of protein solution and 1 μL of reservoir solution containing 16% PEG 600 and 200 mM ammonium phosphate, pH 7.0. The crystals were first characterized using an R-axis 1V++ image plate detector (Rigaku Corp, Tokyo, Japan); diffraction data to 3.2 Å resolution were collected at the Stanford Synchrotron Radiation Lightsource on beam lines 9-2.

Preparation of Chimeric GPIbαN-Long. To check if FIIa binding to surface-anchored GPIbα-N is affected by the spatial orientation of the molecule relative to the surface, we used a recombinant chimeric protein formed by residues −2 to 288 of GPIbα followed by 132 residues of the SV40 large T antigen; this molecule was designated GPIbαN-Long. We generated a monoclonal antibody (LJ-3A2) that reacted specifically with the extended SV40 sequence and not with GPIbα-N; this was used in experiments based on receptor immobilization as an alternative to using LJ-P3 specific for an epitope located in the NH2-terminal region of GPIbα-N.

Evaluation of FIIa Binding to GPIbα-N by Complex Formation in Solution and by SPR. To measure the amount of soluble complex formed, different GPIbα-N species and P-FIIa were mixed in a 3:1 mass ratio and incubated at 37 °C for 30 min. The components of the mixtures were then separated by GPC using two high performance liquid chromatography (HPLC) Superdex columns in series, the first packed with S75 and the second with S200 (GE Healthcare). As a reference, corresponding amounts of the individual complex components were analyzed under the same conditions. Fractions were collected and analyzed for GPIbα-N and P-FIIa content by reversed-phase HPLC, using a 0.2 × 11 cm column packed with 10 μm Poros RH-1 beads (Applied Biosystems, Foster, CA) and, as the eluant, a gradient starting with 0.1% trifluoroacetic acid in Milli-Q (Millford, MA) water and ending with 0.1% trifluoroacetic acid in acetonitrile (Fisher Optima, NJ); light absorbance of the effluent was measured at 215 nm and plotted against elution time. Known amounts of purified GPIbα-N and P-FIIa were analyzed individually using the same procedure, and the relation between known protein mass and area under the corresponding absorption peak provided the calibration to measure unknown quantities of the same protein. The fractions containing P-FIIa bound to GPIbα-N or control P-FIIa not incubated with GPIbα-N did not overlap; thus, the amount of complex formed was expressed as percent P-FIIa present in the former relative to the amount present in the latter. With the excess GPIbα-N used, typically >95% P-FIIa was in the complex fractions.

To generate SPR sensorgrams, GPIbα-N was diluted in HBS containing 3 mM EDTA and 0.005% P20 surfactant (HBS-EP), and injected over one of the chip flow cells to which the antibody LJ-P3 was covalently bound. Injection at a flow rate of 40 μL/min continued until the desired ligand concentration at the chip surface (measured in Biacore Units, RU; 1 RU = 1×10^{-6} Refractive Index Units) was reached. P-FIIa diluted in HBS-EP (concentration range 3.125–10,000 nM) was then injected over the flow cell with bound GPIbα and a control cell where only LJ-P3 was on the surface (nonspecific binding). Association was followed for 3 min, after which HBS-EP was injected for 5 min to assess dissociation. Two 1-min pulses of 3.2 mM NaOH, pH 11.5, were injected at 60 μL/min to detach LJ-P3-bound GPIbα-N before reusing the chip. Binding at saturation (B_{max}) and equilibrium dissociation constant (K_D, binding affinity) were obtained by nonlinear fitting of specific binding (ΔRU, the difference in P-FIIa RU on the surface with and without immobilized GPIbα-N at equilibrium) as a function of P-FIIa concentration; a one-site model of interaction yielded consistently the best fitting (GraphPad Prism version 5.0; GraphPad Software, San Diego, CA). B_{max} was reported as molar ratio of bound P-FIIa and GPIbα-N immobilized onto the chip, the latter calculated with the assumption that 1 RU measured by SPR corresponds to 1 pg of protein/mm^2 of surface. To derive the kinetics rate constants, we assumed that the dissociation phase followed an exponential model and derived the dissociation rate constant (off-rate, k_d) by nonlinear regression fitting of the experimental data using the equation:

$$B_t = \mathrm{NS} + (B_0 - \mathrm{NS}) \cdot e^{-k_d \cdot t} \qquad \textbf{[S1]}$$

Where t is time, B_t is observed binding at time = t, NS is nonspecific binding, and B_0 is total binding at time = 0 (before dissociation begins). Then, the association rate constant (on-rate, k_a) was obtained by nonlinear regression fitting of the association data using the equation:

$$B_t = B_{\mathrm{Eq}} \cdot (1 - e^{-k_{\mathrm{ob}} \cdot t}) \quad \textbf{[S2]}$$

Where B_t is binding at time $= t$, B_{Eq} is maximum (equilibrium) binding measured at any given analyte concentration, and k_{ob} (expressed in units of inverse time) is a constant expressing how quickly binding reaches equilibrium; then, k_a was derived from k_{ob} using the equation:

$$k_a = (k_{\mathrm{ob}} - k_d)/[\mathrm{Analyte}] \quad \textbf{[S3]}$$

Where k_d is the calculated dissociation rate constant.

FIIa Binding to Platelets. Following an institutionally approved protocol, human blood was obtained from healthy donors who gave their informed consent according to the Declaration of Helsinki. Blood (five parts) collected in acid-citrate-dextrose (1 part; 71 mM citric acid, 85 mM sodium citrate, 111 mM dextrose, pH 4.5) was centrifuged at 600 g for 12 min to prepare platelet-rich plasma. A platelet pellet was then obtained by centrifuging platelet-rich plasma at 800 g for 15 min in the presence of 10 mM PG E_1 (Enzo Life sciences, Farmingdale, NY) and 0.6 U/mL Apyrase Grade VII (Sigma). The pellet was washed once by resuspension and centrifugation in modified Tyrode buffer, pH 6.5 (135 mM sodium chloride, 2.9 mM magnesium chloride, 1 mM sodium phosphate monobasic, 10 mM Hepes , 2.5 mM dextrose), and finally resuspended in the same buffer but at pH 7.4; the platelet count was adjusted to $2 \cdot 10^7$/mL. For these assays, FIIa was blocked in the active site with biotin-PPACK (B-P-FIIa; Haematologic Technologies) and characterized as described above for P-FIIa. In initial assays, B-P-FIIa was added at the desired concentration (maximum 800 nM) into aliquots of the platelet suspension and incubated for the indicated time at room temperature (22–25 °C), followed by phycoerythrin-conjugated streptavidin (S-PE; Invitrogen; 1.25 μg/mL) for 5 min; in subsequent experiments (see Fig. S5*C*), B-P-FIIa and S-PE were mixed at a fixed molar ratio (4 : 1) before addition to platelets. The two methods gave similar results, but the latter was more reproducible and was used for evaluating the time-course of binding. When indicated, the anti-GPIbα monoclonal antibody, LJ-Ib10 (2), which specifically inhibits FIIa binding (3), was added to the platelet suspension five minutes before the addition of S-PE/B-P-FIIa. Binding was measured by flow-cytometry, without sample dilution, using a FACS Calibur II equipped with a 488 nm argon laser and the software CellQuest for data evaluation (Becton Dickinson and Company, Franklin Lakes, NJ). Results were expressed as geometric mean of the fluorescence intensity of 10,000 events and analyzed with GraphPad Prism version 5.0.

Additional Materials Used in Supporting Experiments. In addition to DNA aptamers, we used other FIIa exosite inhibitors to evaluate their effect on binding to GPIbα. Lepirudin (recombinant [Leu^1-Thr^2]-63-desulfohirudin; Refludan; Bayer Corp., Pharmaceutical Div., West Haven, CT) and hirugen (synthetic 3-O-sulfo-Tyr^{63}-hirudin [54–65]; Anaspec, Fremont, CA) were used to block exosite I; heparin (sodium salt, Grade II, from porcine intestinal mucosa; Sigma-Aldrich Co., St. Louis, MO) to block exosite II. Alexa Fluor 488-conjugated streptavidin was from Invitrogen, Carlsbad, CA.

Evaluation of Results Obtained with Inhibitors of FIIa Binding to GPIbα. The inhibition constants (K_i) of FIIa exosite inhibitors were calculated according to the Cheng-Prusoff equation (4) from the corresponding IC_{50} values derived from inhibition dose-response curves fitted with GraphPad Prism (version 5.0; GraphPad Software, San Diego, CA). Results were expressed as mean ± SEM of at least two independent determinations.

1. Celikel R, et al. (2003) Modulation of α-thrombin function by distinct interactions with platelet glycoprotein Ibα. *Science* 301:218–221.
2. Handa M, Titani K, Holland LZ, Roberts JR, Ruggeri ZM (1986) The von Willebrand factor-binding domain of platelet membrane glycoprotein Ib. Characterization by monoclonal antibodies and partial amino acid sequence analysis of proteolytic fragments. *J Biol Chem* 261:12579–12585.
3. De Marco L, Mazzucato M, Masotti A, Fenton JW, II, Ruggeri ZM (1991) Function of glycoprotein Ibα in platelet activation induced by α-thrombin. *J Biol Chem* 266:23776–23783.
4. Cheng Y, Prusoff WH (1973) Relationship between the inhibition constant (K_i) and the concentration of inhibitor which causes 50 per cent inhibition (i50) of an enzymatic reaction. *Biochem Pharmacol* 22:3099–3108.

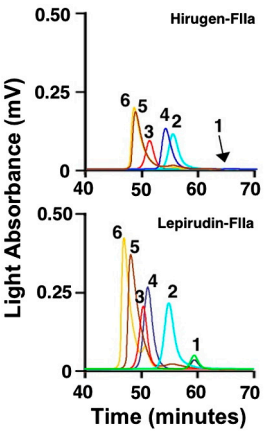

Fig. S1. Exosite I-specific ligands fail to inhibit P-FIIa binding to soluble GPIbα-N. Top. Elution time from a GPC column of P-FIIa (peak 2); wild type GPIbα-N (peak 3); P-FIIa plus hirugen (8-fold molar excess; peak 4); P-FIIa plus GPIbα-N (peak 5); and hirugen plus P-FIIa plus GPIbα-N (peak 6). Mixtures yielding new peaks eluting earlier than individual components indicates complex formation in solution. Note that hirugen alone (peak 1) has no significant absorption under these experimental conditions. Bottom. The same as above, but using lepirudin (peak 1) instead of hirugen and FIIa instead of P-FIIa; lepirudin has a larger molecular mass than hirugen, thus the positional shift of peak 6 as compared to peak 5 is more evident.

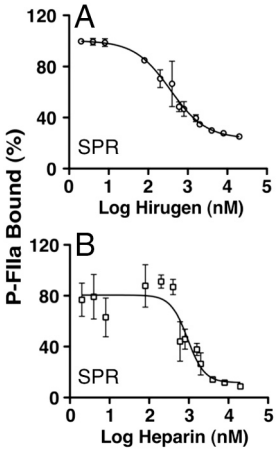

Fig. S2. Inhibition of P-FIIa binding to immobilized GPIbα-N by hirugen and heparin. (*A*). SPR analysis of the inhibition of P-FIIa (used at K_D concentration, 80 nM) binding to immobilized wild type GPIbα-N peak 3 by hirugen; the calculated K_i was 178.6 ± 0.6 nM. (*B*).The same as in *A*, but using the exosite II inhibitor, heparin; the calculated K_i was 464.5 ± 3.9 nM. Results are expressed as percent binding relative to a control without inhibitor.

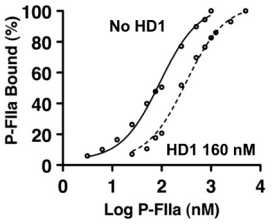

Fig. S3. Competitive inhibition of P-FIIa binding to immobilized GPIbα-N by HD1. SPR analysis of dose-dependent P-FIIa binding to immobilized wild type GPIbα-N peak 3 with or without HD1 added at approximately IC_{50} concentration (see Fig. 5*A*). Results are expressed as percent binding relative to that measured at the highest concentration of P-FIIa added. The apparent K_D (250 nM) calculated from the fitting of FIIa binding in the presence of HD1 is in agreement with a model of competitive antagonism according to the equation: $K_{Dapp} = K_D(1 + [\text{Inhibitor}]/K_i)$, where K_{Dapp} and K_D are the equilibrium dissociation constants in the presence and absence of inhibitor, respectively. Indeed, substituting in the equation the values for $K_D = 76$ nM (Table 2); $K_i = 77.3$ nM (Fig. 5*A*), then $K_{Dapp} = 233.31$ nM.

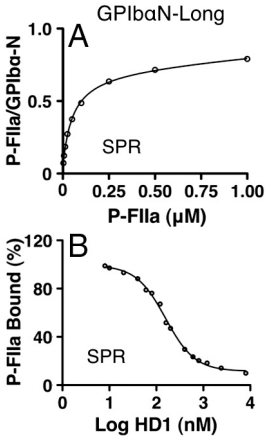

Fig. S4. Inhibition of P-FIIa binding to immobilized GPIbαN-Long by HD1. (*A*). Dose-response of P-FIIa binding to fully sulfated GPIbαN-Long measured by SPR. Binding is reported as mole of P-FIIa bound per mole of GPIbαN-Long immobilized onto the chip. (*B*). Inhibition of P-FIIa binding (used at K_D concentration) to immobilized GPIbαN-Long by exosite I-specific aptamer HD1. Results are expressed as binding in percent of a control with no inhibitor. The corresponding IC_{50} and K_i values (nM; mean ± standard error of the mean; $n = 2$), respectively, were: 156.5 ± 1.02 and 67.07 ± 0.58.

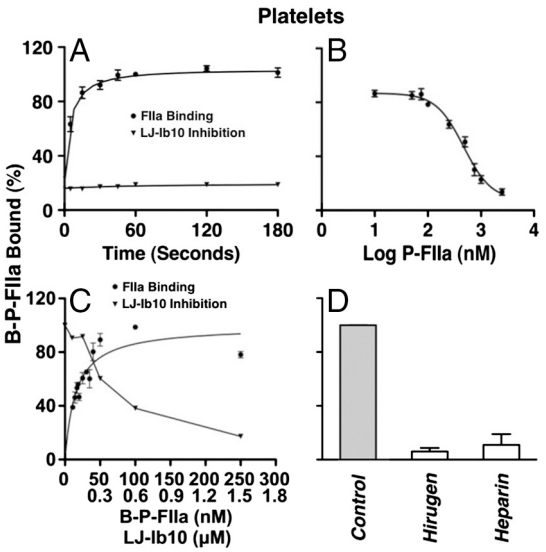

Fig. S5. B-P-FIIa binding to human platelets and inhibition by hirugen and heparin. (*A*). Time course of B-P-FIIa (used at K_D concentration) binding to washed human platelets ($2 \cdot 10^7$ platelets/mL) with or without addition of the anti-human GPIbα monoclonal antibody, LJ-Ib10 (50 μg/mL). Alexa Fluor 488-conjugated streptavidin (0.25 molar ratio) was mixed with B-P-FIIa before adding to the platelet suspension. After incubation at room temperature (22–25 °C) for the indicated time periods, samples were analyzed by flow cytometry without dilution. Results are expressed as geometric mean of the fluorescence of 10,000 measured events. (*B*). Experiment performed as in *A* except that, after incubation of B-P-FIIa/Alexa Fluor 488-conjugated streptavidin with platelets for 20 min, increasing concentrations of P-FIIa, as indicated, were added. After additional 20 min, the displacement of B-P-FIIa was evaluated by flow cytometry. Results are reported as percent residual binding relative to that measured before the addition of P-FIIa. (*C*). Dose-response curves of B-P-FIIa binding to platelets and of the inhibition by increasing concentrations of LJ-Ib10; in the latter experiment, B-P-FIIa was used at 100 nM. Mixtures were incubated for 20 min at room temperature. (*D*). B-P-FIIa was used at saturating concentration and binding in the presence of 10-fold molar excess of exosite I-specific hirugen or exosite II-specific heparin (average molecular weight 15 kDa) was evaluated after 20 min at room temperature. In (*C* and *D*) detection was by PE-conjugated streptavidin.

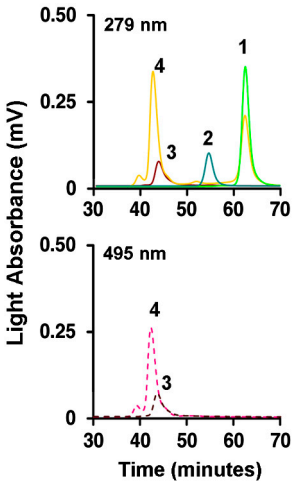

Fig. S6. Stable association of Alexa Fluor 488-streptavidin with B-P-FIIa. Top. Elution time from a GPC column of HD1 (peak 1), B-P-FIIa (peak 2), B-P-FIIa/Alexa Fluor 488-streptavidin (peak 3), or B-P-FIIa/ Alexa Fluor 488 streptavidin (1 : 1 molar ratio) in the presence of a 9-fold molar excess HD1 (peak 4). Light transmittance measured at 279 nm to detect protein. Bottom. Light transmittance measured at 495 nm, corresponding to the maximum absorption peak of the fluorochrome. Note that the volume analyzed for different mixtures was not constant.

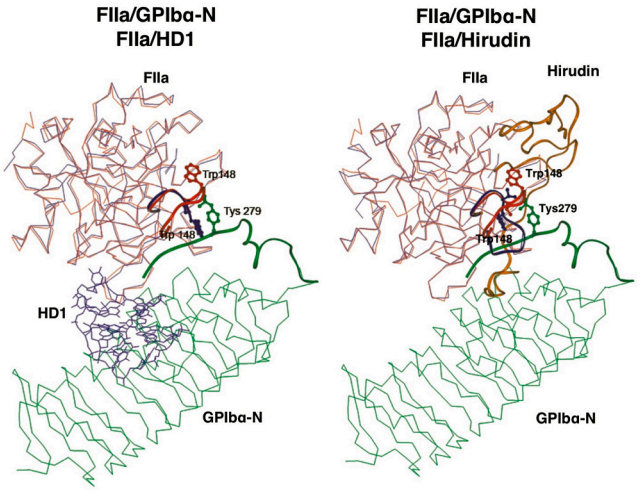

Fig. S7. HD1 and hirudin prevent the interaction of GPIbα-N Tys^{279} with FIIa Trp^{148}. Superposition of the crystal structures of the complex of FIIa with fully sulfated GPIbα-N (PDB ID: 3PMH) and FIIa in complex with HD1 (left, PDB ID: 1HUT) or hirudin (right, PDB ID: 2HTC). In the FIIa/ GPIbα-N complex, Tys^{279} anchors a string of negatively charged GPIbα residues (279–284) to FIIa by interacting with the backbone of Trp^{148} flanking exosite I. This interaction is unattainable when Tyr^{279} is substituted by Phe or the position of Trp^{148} is changed upon binding of the two exosite I ligands. GPIbα-N is colored green; FIIa is red in complex with GPIbα-N and blue in complex with HD1 or hirudin; the latter two are light blue and dark orange, respectively. Tys^{279} in GPIbα-N and Thr^{147} /Trp^{148} in FIIa are shown with side chains in stick and ball representation.

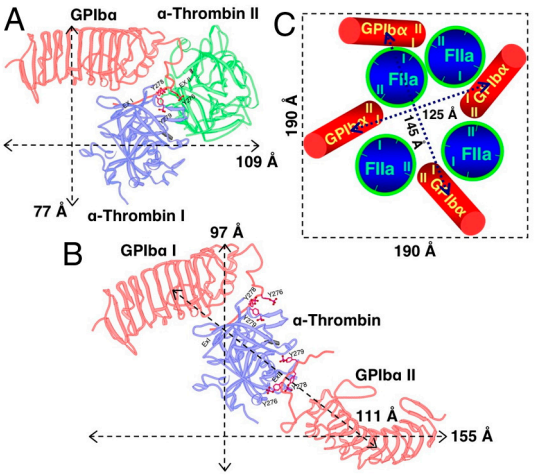

Fig. S8. Schematic representation of the mechanism of FIIa binding to platelets based on crystal structure information. (*A*). Structure of the complex showing the contacts between one GPIbα-N (receptor) and two FIIa (ligand) molecules. (*B*). Structure of the complex showing the contacts between one FIIa and two GPIbα-N molecules. This mode of interaction is required for stable association of the ligand with the immobilized receptor. (*C*). Schematic representation of a spatial arrangement, compatible with molecular dimensions in the crystal and 1 : 1 stoichiometry, in which each of four ligand molecules is bound concurrently to two receptors through distinct sites, and each receptor binds two distinct ligands. The indicated distances between the centroids of receptor molecules are estimates based on the proposed clustering and compatible with the proposed binding mechanism.

Table S1. Contact distances (in Å) between sulfate oxygen atoms of three sulfated Tyr residues of GPIbα and atoms of residues in FIIa site I and site II

Sulfate oxygen atoms of GP Ibα	Site I contacts (exosite I)		Site II contacts (exosite II)	
Tys276-O1			Arg126-NH1	3.69
Tys276-O2			Arg126-CG	3.29
			Arg126-CD	3.76
			Arg126-NE	3.83
			Phe232-CE1	3.23
			Phe232-CZ	3.03
			Arg126-CZ	3.41
			Arg126-NH1	2.65
Tys276-O3	Asp60e-CG	3.89	Arg126-CG	3.13
	Asp60e-O	3.15	Arg126-CD	3.92
	Asp60e-CB	3.68	Arg126-NE	3.71
			Arg126-CZ	3.71
			Arg126-NH1	3.82
Tys278-O1	none		none	
Tys278-O2	Pro37-CD	2.85		
	Pro37-CB	3.35		
	PRO37-CG	2.65		
Tys278-O3	Arg35-CZ	3.84	Lys236-NZ	3.46
	Arg35-NH1	3.31		
	Arg35-NH2	3.80		
Tys279-O1	Thr147-OG1	3.79		
	Thr147-CG2	3.00		
	Thr147-CB	3.99		
Tys279-O2	Thr147-CG2	3.74	Trp237-CD1	3.63
	Thr147-C	3.23		
	Thr147-O	3.09		
	Trp148-N	3.10		
	Trp148-CA	2.75		
	Trp148-CB	3.36		
	Trp148-C	3.92		
Tys279-O3			Lys240-CG	3.74
			Lys240-NZ	3.49

Hydrophilic contacts are underlined.